Engineering Science & Technology
http://ojs.wiserpub.com/index.php/EST/

UNIVERSAL WISER PUBLISHER

Research Article

Pedalling Comfort of a Custom Pedal Series Hybrid Drivetrain in a Cargo E-Tricycle

Jordi D'hondt[1*], Peter Slaets[2], Eric Demeester[3], Marc Juwet[1]

[1]KU Leuven, Department of Robotics, Automation and Mechatronics, Gebroeders de Smetstraat 1, 9000 Gent, Belgium
[2]KU Leuven, Department of Robotics, Automation and Mechatronics, Andreas Vesaliusstraat 13-box 2600, 3000 Leuven, Belgium
[3]KU Leuven, Department of Robotics, Automation and Mechatronics, Wetenschapspark 27-box 15152, 3590 Diepenbeek, Belgium
Email: Jordi.dhondt@kuleuven.be

Received: 24 February 2022; **Revised:** 18 June 2022; **Accepted:** 27 June 2022

Abstract: A Pedal Series Hybrid Drivetrain (PSHD) uses an electrical power transmission rather than a chain, belt, or shaft. It creates exciting opportunities for the vehicle's design, but pedalling does not always feel comfortable. This study evaluates the pedalling comfort of a custom PSHD in an electric cargo tricycle. In this PSHD, pedal-driven generator converts human mechanical power to electrical power that is used by two hub motors to propel the vehicle. The pedal-driven generator is mechanically decoupled from the propulsion of the vehicle. Therefore, natural pedalling is replicated using a custom programmable controller for the mechanical resistance of the generator. Test subjects reported a very comfortable pedalling feeling, however slightly different from the feeling of a traditional e-bike. They failed to explain the differences in more detail. Further measurements show that the pedal generator of the PSHD has the same power cycle as the pedals in a traditional e-bike, but the pedal generator has a greater variation in the instantaneous angular velocity.

***Keywords*:** pedal series hybrid drivetrain, cargo bike, pedal forces, pedal generator, instantaneous angular velocity

1. Introduction

A new concept vehicle for last-mile delivery in city centres has been developed [1]. A custom Pedal Series Hybrid Drivetrain (PSHD) was used as the means of propulsion. This drivetrain powers the vehicle using pedal-generated energy and battery-stored energy. The pedals drive a generator mounted on the bottom bracket of the tricycle. Both rear wheels of the tricycle include an electrical wheel motor. The battery is electrically connected to the motors and the generator.

The lack of a conventional mechanical transmission, including a chain, belt, or shaft, reduces the overall design constraints for the vehicle. Maintenance interventions are expected to be reduced as well. However, a successful market introduction of such a PSHD cargo tricycle also depends on its acceptance by the couriers. A natural feeling of pedalling is a major prerequisite. Therefore, the generator resistance should vary during a revolution of the pedals. A programmable resistance controller is developed. The control loop uses the angular pedal velocity as a primary parameter and is further finetuned using the propulsion setpoints of the vehicle.

The technology, advantages, disadvantages, and examples of PSHD on the one hand, and the state of the art in

DOI: https://doi.org/10.37256/est.3220221376

pedalling mechanics measurements on the other hand, are described to illustrate the context and purpose of the study.

2. Pedal series hybrid drivetrain

Traditional bicycles are powered only by the energy of the cyclist applied on the pedals. It is transferred to the rear wheel by a chain transmission or something similar. Only mechanical energy was used for the propulsion. Conventional e-bikes have an electric motor to assist the cyclist. The assistance motor is a mid-drive motor mounted at the bottom bracket or a hub motor in the front- or rear wheel. E-bikes use the same cyclist power but are also electrically assisted. The electrical assistance and human power work in parallel. Therefore, the drivetrain in such an e-bike is called a Pedal Parallel Hybrid Drivetrain. In a Pedal Series Hybrid Drivetrain (PSHD), there is no mechanical transmission between the pedals and the wheels. The only power transmission is electrical. The pedals are connected to a generator that converts human power to electrical energy [2]. This electric energy is stored in batteries or capacitors or is used directly by one or more motors that propel the vehicle. Most motors can be used, but Brush Less Direct Current (BLDC) hub motors integrated into a wheel are the most common. This energy flow can be seen in Figure 1.

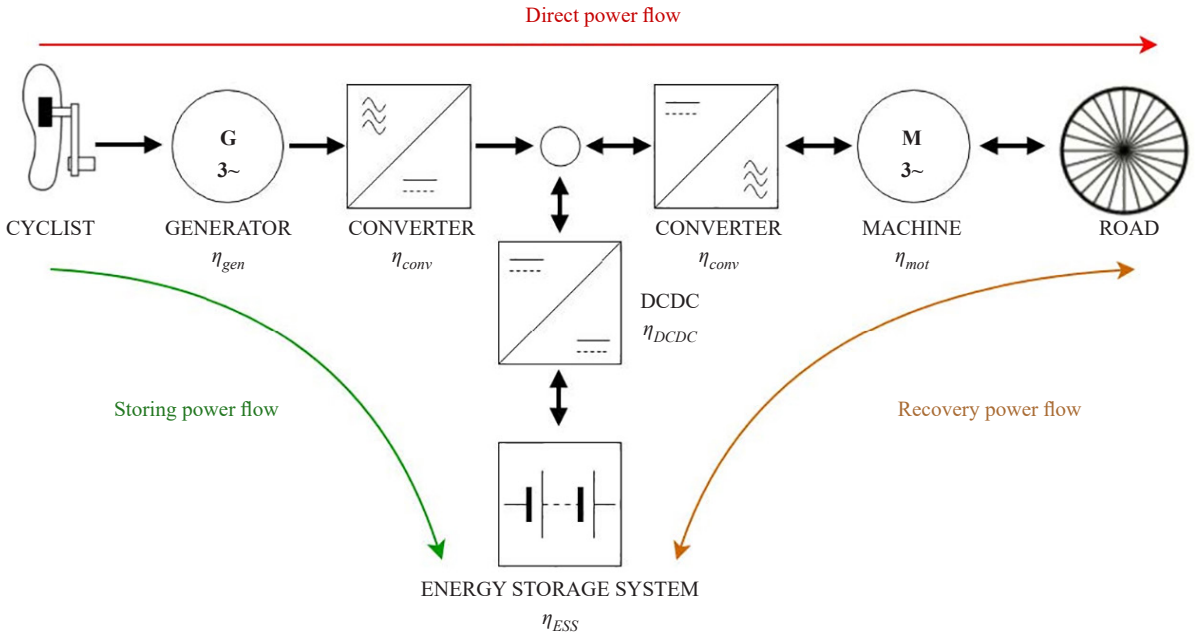

Figure 1. Pedal Series Hybrid workings [3]

2.1 *Advantages*

The PSHD also has multiple advantages. The use of a PSHD is maintenance-friendly [4]. The generator and the hub motors are both BLDC motors. These types of motors are very low maintenance [5]. A conventional e-bike uses a chain that requires a lot of maintenance and is one of the components most vulnerable to wear. Furthermore, the majority of E-bikes are assisted using a mid-drive. This configuration transfers the human pedal and drive power through the chain. The combined power causes extra stress on the chain and increases the chance of failure. An alternative that is less susceptible to wear or failure is belt-drive, which is more expensive. The PSHD drivetrain reduces the maintenance costs and is less likely to break down.

An electrical drivetrain has fewer design constraints compared to a traditional chain transmission. The lack of a mechanical transmission creates more design possibilities. Only a flexible electrical cable is required to connect the

generator with the propulsion. This "cycle by wire" connection requires no alignment and doesn't require room for a mechanical connection to the rear wheels. Without a mechanical transmission, the wheel dropout can be smaller, resulting in a narrower vehicle. The improvement of design constraints doesn't specifically benefit conventional bikes as they have evolved with a traditional chain drivetrain. Furthermore, the drivetrain can operate with a virtual Continuous Variable Transmission (CVT) without using complex mechanical components. This allows the pedal generator to be used constantly at the most comfortable cadence independent of the vehicle's speed, even while departing. E-bikes that use a rotation sensor must depart on full human power before the assistance begins. These features make the PSHD very ergonomic.

Recumbent bicycles have a long chain from the pedals to the rear wheel as a drivetrain. They have a fixed seat and an adjustable bottom bracket to fit the cyclist's length. Adjusting the position of the bottom bracket also requires an adjustment of the chain length, while an electrical drivetrain requires no extra adjustment. This drivetrain can also be used in tandem. A conventional tandem utilises two bottom brackets which are synchronized using a chain. As a result, the cyclist must pedal at the same cadence. Replacing at least one pedal crank with a pedal generator allows both cyclists to pedal at their comfortable cadence.

PSHD makes pedalling stationary possible to recharge the battery, as presented in the Lean Mean Machine [6]. This is only the case for multitrack vehicles that remain upright while stationary.

2.2 *Disadvantages*

PSHD is an uncommon drivetrain. This doesn't often occur since it has multiple disadvantages. This type of drivetrain requires a generator and a motor. These components can be more expensive compared with the required parts on a conventional e-bike. However, if the e-bike is equipped with internal hub gears or CVT gearing, which is implemented in the PSHD drivetrain, the cost can be similar [4]. Hub motors have limited torque, and the PSHD doesn't receive additional torque from the pedals. European regulations limit the nominal continuous power of e-bikes to 250 W [7]. The motor power may be insufficient in uphill terrain for fully loaded cargo bikes without the additional cyclist power that can provide high torque at low speed. Furthermore, the pedal generator requires a custom control to experience a natural cycling feeling. If the pedal generator doesn't have a natural pedalling feeling, the vehicle won't be comfortable and won't be used.

2.3 *Examples of PSHD*

There are only a few examples of vehicles using a PSHD, although the concept was patented in 1975 [2]. The Mando Footloose is presented in 2013 and uses a pedal generator and a rear-wheel BLDC motor. The lack of a chain allows for a unique, easily foldable design, as seen in Figure 2. The innovative design even won the "2013 red dot design award" [8]. However, due to the limited power and a noisy motor, the bicycle wasn't a success.

Figure 2. Mando footloose [8]

The Tortuga XL is a cargo bike using a PSHD and was presented in 2016 as seen in Figure 3. The cargo bike has a high cargo capacity. However, the vehicle's pedal generator has no variable resistance. The uncomfortable pedalling feeling explains why the vehicle was not successful.

Figure 3. Tortuga XL [9]

A tadpole (two wheels in front) recumbent tricycle was built and tested in 2020 during the France Sun Trip [10], [12]. On top of the pedal generator, PV solar panels are used for power generation. Capacitors are used for energy storage (Figure 4a). A 1 kW hub motor is mounted in the rear wheel. The mechanical decoupling of the pedals and wheels allows the cyclist to keep pedalling without additional effort in mountainous terrain. It also allows the vehicle to be pedalled stationary.

The recumbent tricycle of Bernard Cauquil also participated in the Sun Trip (Figure 4b). This delta tricycle uses a 1 kW hub motor in the front wheel [13], [14].

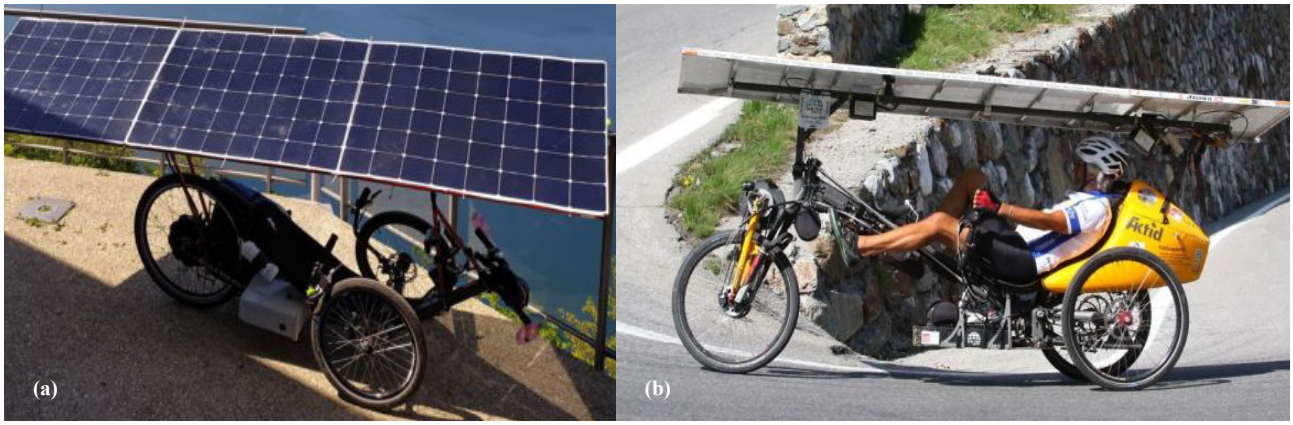

Figure 4. (a) vehicle of Edgar Tournon [11]; (b) Bernard Cauquil [14]

Another example uses 12 pedal generators that all work independently as seen in Figure 5. All cyclists can pedal in their comfortable cadence. This vehicle is being tested in Le Teil, France [15].

Figure 5. bicycle bus [15]

The above examples use custom-developed drivetrains. Mando developed the Smart Personal Mobility (SPM) (Figure 6a) and Schaeffler developed the free drive (Figure 6b) [16], [17].

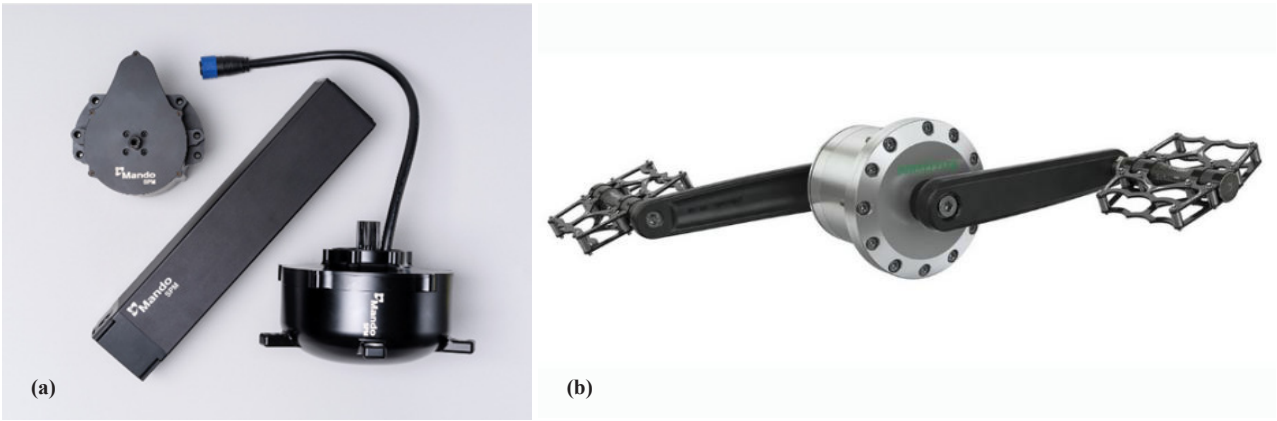

Figure 6. (a) Mando SPM [16]; (b) Schaeffler free drive [17]

2.4 *Pedal Properties*

To ride a bicycle, numerous actions are needed. Cyclists have to maintain balance by steering and leaning whilst cycling. At the same time, they have to apply force on the pedals for propulsion. These actions are automatically performed after enough practice. Maintaining balance is aided by the self-stabilizing properties of a bicycle. It even allows cyclists to ride without hands on the handlebars. These self-stabilizing properties have been researched thoroughly [18]-[25]. It depends, among other things, on the caster of the fork and the gyroscopic effects of the wheels. The complete geometry and mass of the vehicle have further influence. The effect varies with the bicycle's velocity. The stability of a bicycle can be simulated using the Carvallo-Whipple model [20].

Although the cyclists interact with their seats, handlebars, and pedals [26]-[29], the majority of the cyclist/bicycle interaction research is focused on the global forces exerted on the pedals since this creates the propulsion [29]-[34]. Research reveals the force applied on the pedals varies according to the orientation of the pedal cranks. These variations are due to the biomechanical structure of the human leg [35], [36]. A leg can generate a high downward force but can only to create a limited horizontal force. Since the feet are not fixed on a standard pedal, no upward force can be applied to the pedals. The feasible forces of the leg can be seen in Figure 7.

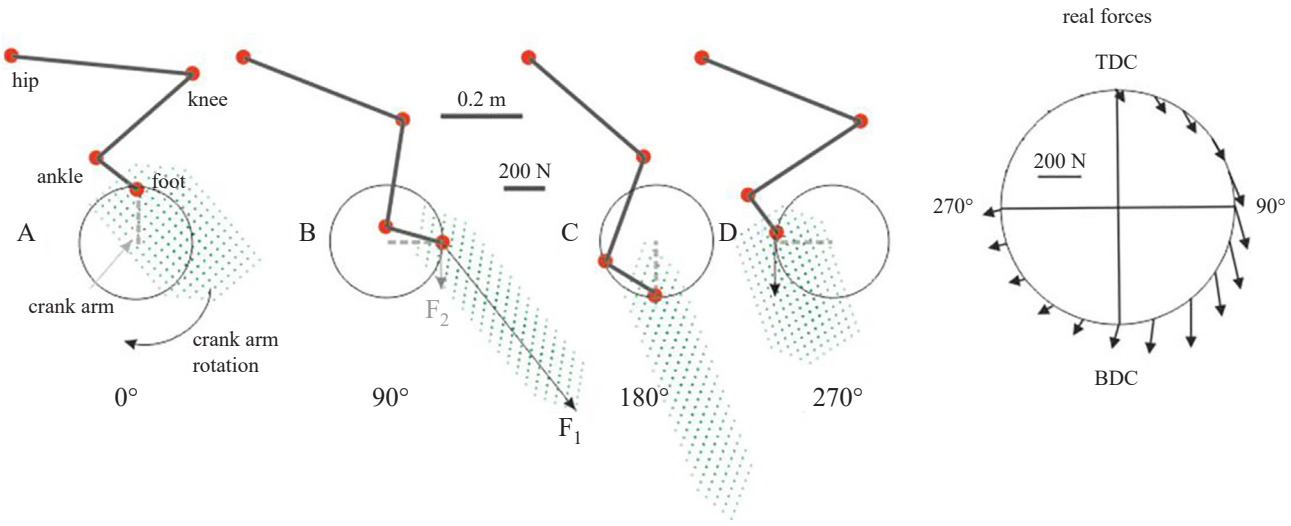

Figure 7. Set of feasible forces at different crank angles [35]

This corresponds to pedal measurements [29], [31]-[34]. The highest force is applied during the downward pedal movement [30]. During the horizontal and upward pedal movement, the cyclist can not apply a useful force on a traditional bicycle, as can be seen in Figure 8.

Since the pedals alternate, the upward movement of one pedal is covered by the downward movement of the other pedal. Around the horizontal pedal movement, corresponding to a vertical pedal crank orientation, little to no force is applied by both legs. These vertical pedal crank orientations are therefore called dead centres. They are however easily overcome due to the bicycle's inertia. The force can be converted to torque and the dead centres are also clearly visible in Figure 9.

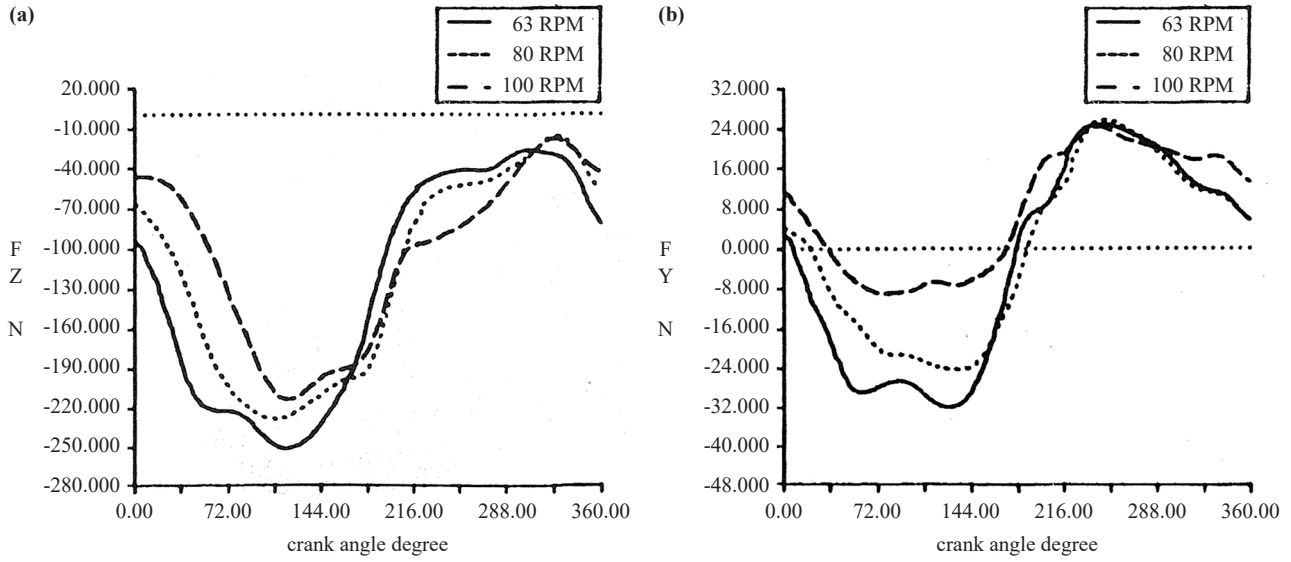

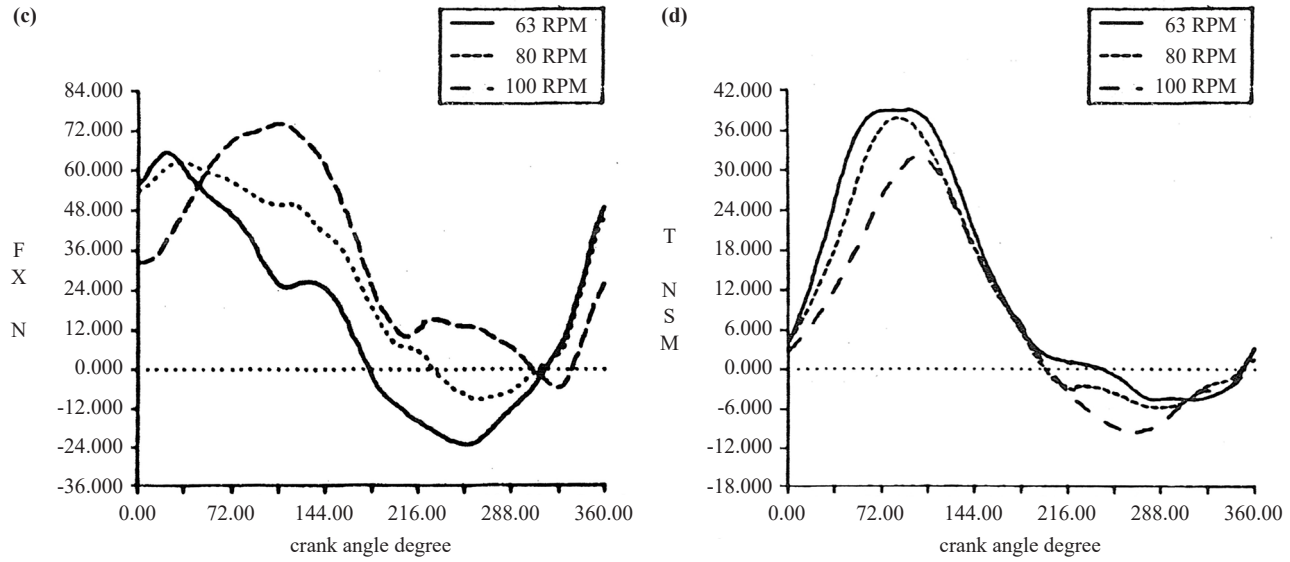

Figure 8. right pedal forces and torque profiles (a) Fz (b) Fy (c) Fx (d) torque with 0° being the upward pedal position [31]

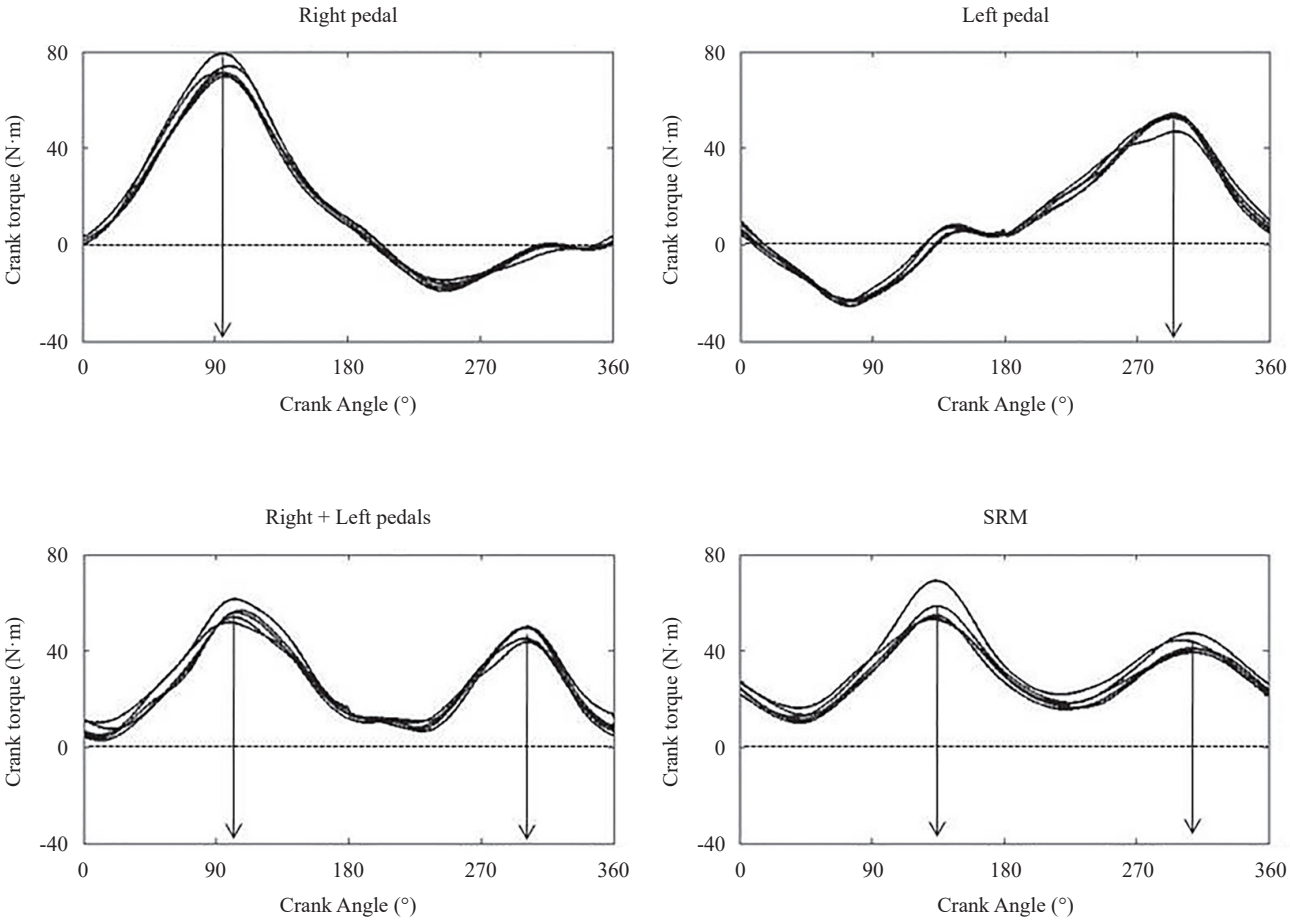

Figure 9. Crank torque measurement by the pedals and SRM torque analysis [32]

The variation in the crank torque shows two peaks in one rotation each created by one pedal. The two minima represent the dead centres. Although the bicycle's inertia overcomes the dead centres, this can still cause a small momentarily angular decrease of the pedal cranks. An angular velocity increase can occur during the torque peaks.

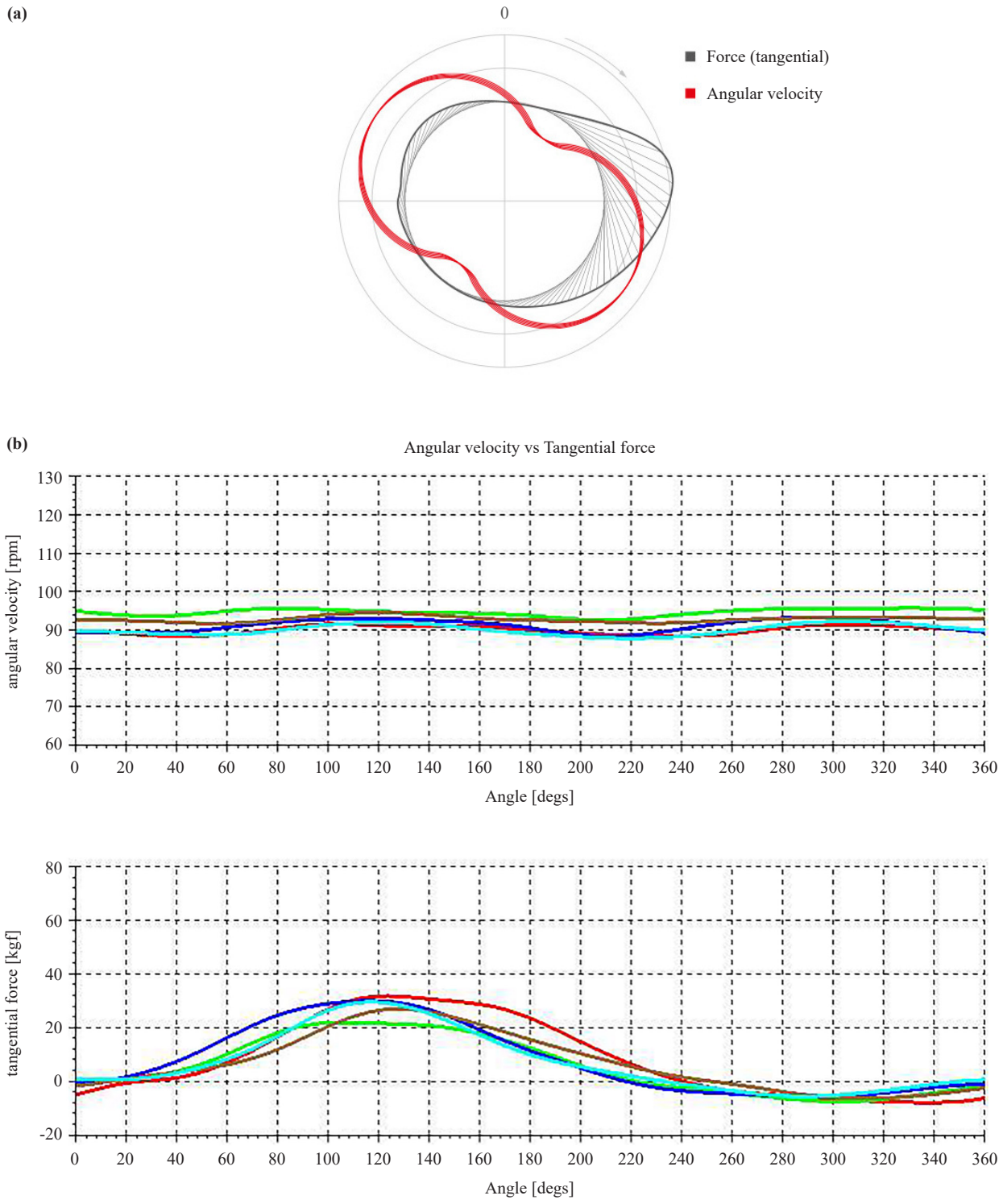

Figure 10. (a) Force and angular velocity of IAV power meter [37]; (b) angular velocity and tangential force of a single pedal revolution of 5 different cyclists [38]

The majority of research assumes that the difference between the Instantaneous Angular Velocity (IAV) and the average pedalling cadence is negligible and is therefore rarely mentioned. Force and torque measurements don't require an angular velocity but should know the crank orientation. These orientations are often interpolated using the cadence. Power meters also require an angular velocity. Current power meters utilize the average cadence, which can cause a miscalculation. Favero Electronics developed an IAV Power meter [37] to improve the accuracy (Figure 10a). Their research noticed an IAV variation while cycling on a flat road between 5% and 10% (Figure 10b). This variation can cause a power miscalculation as high as 1.6%. The difference can be significantly greater under certain conditions such as on a stationary trainer due to the lower inertia or when using an oval chain ring.

3. Research objectives

Although the PSHD concept has been known since 1975 [2], no significant penetration of this type of drivetrain has been observed in the market. The main objective of this research is to prove the suitability of a PSHD as an alternative drivetrain for bicycles. To reach this objective, it should be shown that the three primary disadvantages of a PSHD are irrelevant or can be overcome:

- a PSHD should have a natural or comfortable pedalling feeling.
- the generator can serve as an electrical gearbox, reducing mechanical components such as a derailleur, internal hub gearbox, or something similar.
- the cyclist should experience unfavourable driving conditions such as driving fully loaded, driving uphill, driving into a headwind, … and have the choice to add more power under such conditions.

4. Tricycle description

The vehicle used in this research is a tilting delta tricycle (Figure 11) developed after extensive market research [39]. This cargo bike can carry euro pallet-sized loads with a maximum payload capacity of 250 kg. The vehicle is designed to be stable and manoeuvrable, independent of the payload. The tricycle consists of a tilting front driver module that allows the driver to tilt while manoeuvring, resulting in a comfortable driving feeling [1].

Figure 11. Delta tricycle cargo vehicle

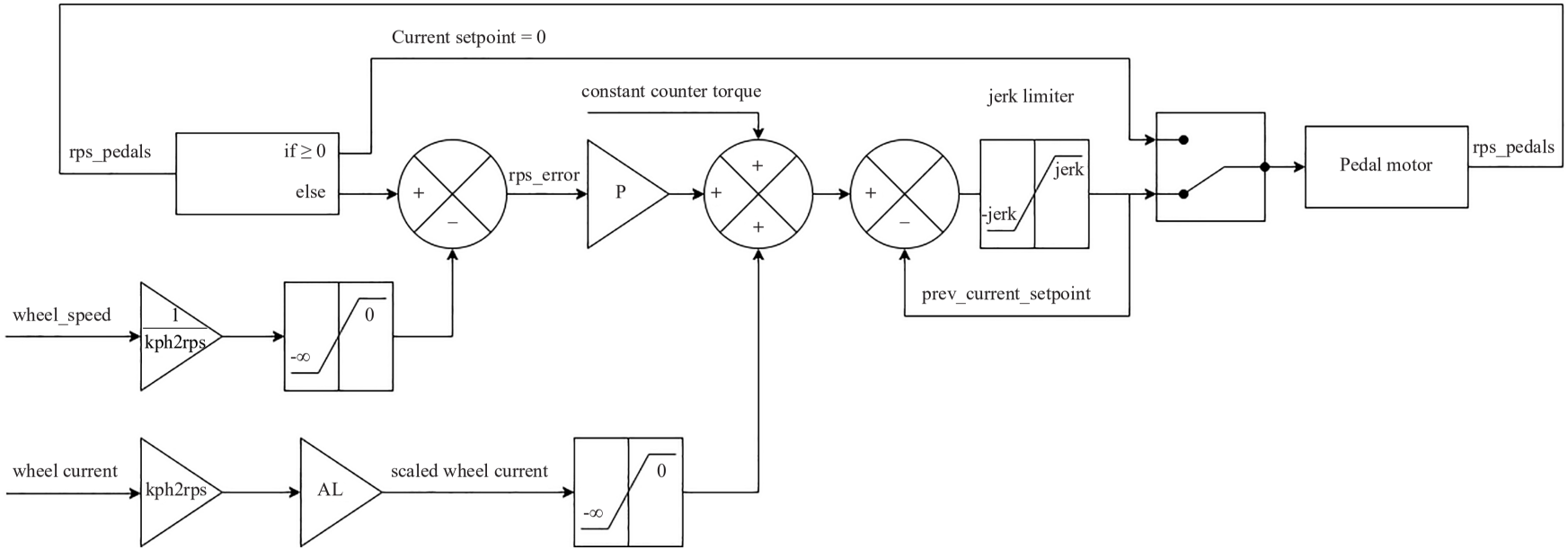

Figure 12. pedal generator control loop

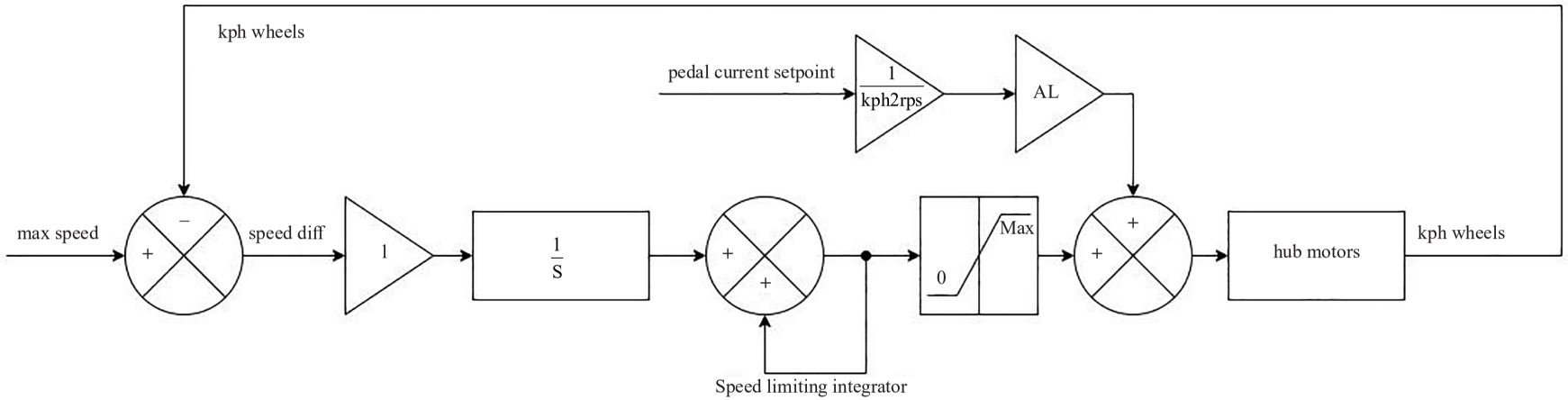

Figure 13. wheel control loop

4.1 *Hardware*

The delta tricycle utilizes a PSHD. Both rear wheels were equipped with a 2000W BLDC hub motor. They have hall sensors for incremental positioning and speed measurements. The generator mounted on the pedal bracket is a 250 W mid-drive motor modified to allow the pedals to drive the BLDC motor. It also uses hall sensors for speed measurements. Custom control hardware and software are used for the generator and both hub motors. An ESP32 data link can connect to a smartphone that serves as a dashboard for a real-time view of velocity, energy consumption, energy storage, settings.

4.2 *Control loop*

Driving the vehicle requires two control loops. One control loop operates the generator, and one control loop operates the hub motors in the wheels. The pedal generator control loop regulates the power generation to achieve a natural pedalling feeling.

In a mechanical drivetrain, a balance is present between the applied pedal power and the acceleration of the vehicle. Increasing the pedal power results in an increase in the vehicle's velocity. Lowering the pedal power decreased the velocity. On the other hand, changes in the environment like an increase in slope require an increase in pedal power to maintain a constant velocity.

The electrical drivetrain simulates this effect through data exchange between the generator and the hub motors. Vehicle speed is derived from the hall sensors in the hub motors (wheel_speed). The average current (wheel_current) of the hub motors indicates the used propulsion.

Wheel_speed is scaled to the rotational speed of the pedals using a virtual gearing (kph2rps). The used hub motor current is scaled using the same virtual gearing. The wheel current is further scaled according to the desired Assistance Level. This results in a scaled amplification factor for the control loop.

The rotational speed difference between the geared wheels and the pedals is proportionally scaled to a current value. A constant counter-torque is added to maintain some small resistance during the dead centre. The scaled wheel current is also added with this and results in a current setpoint. The change in the current setpoint is limited to reducing the jerk in the pedal generator. This control loop can be seen in Figure 12. The control loop results in a natural pedalling experience and gives proportional feedback according to the wheel power. Furthermore, this control system serves as a continuous variable transmission. Gearing changes automatically to provide the driver with a comfortable pedalling cadence.

The control loop for the propulsion is done individually for each hub motor. The control loop receives the pedal current setpoints. The setpoint is scaled using the gearing and the Assistance Level. An integrator of the speed difference between the speed of the hub motor and the maximum velocity is added as a velocity limiter. This results in a current setpoint for the hub motor. The control loop can be seen in Figure 13.

The pedal generator should create a natural feeling without feedback from the pedal crank orientations. The rotational difference between the pedals and the hub motors is used to simulate the inertia present in a traditional drivetrain. However, using the rotational difference requires a noticeable difference with limited gain or the pedal generator would have an uncontrollable oscillating resistance. This can cause a bigger difference in the rotational pedal speed.

5. Methods

The PSHD must create the natural feeling of riding a mechanical drive train. To evaluate and improve this natural feeling, test subjects used the test tricycle and commented on their experiences. The test subjects ranged from 21 to 50 years old and have experience levels ranging from recreational cyclists to professional couriers. While driving the vehicle, data from the pedal generator were measured and stored. These data are compared to data gathered by driving a conventional e-bike.

5.1 *Pedal generator*

The relevant data to evaluate the pedal generator is collected whilst cycling on bicycle lanes. This test collects the motor position, the motor speed and the motor current according to the time. The data is processed to organise the motor speed and the motor current according to the pedal orientation. The values are interpolated to obtain an equal spacing of 1 degree. As both pedal cranks are attached to the same motor shaft, the generated motor current accounts for the force applied on both pedals. This generated current is proportional to the applied tangential force. The motor speed is scaled to the internal gearbox of the pedal generator to obtain the pedal cadence. This pedal cadence is further analysed. The instantaneous cadence is divided by the mean cadence of the same revolution, as seen in formula 1.

$$c_p = \frac{c_i}{c_m} \tag{1}$$

Where:

c_i = instantaneous cadence

c_m = mean cadence

c_p = proportional cadence

The result displays the angular velocity in percentage and shows the variations in the cadence according to the crank orientation.

5.2 *Measurement bicycle*

The pedal generator is compared using the pedal values of a measurement bicycle. The measurement bicycle measures the complete cyclist/bicycle interaction. The bicycle has a 6-dimensional load cell incorporated in the seat post [26] and the handlebar stem [27]. There is also a 3-dimensional load cell in each pedal [29]. The orientation of the pedals and the crank are measured, enabling the calculation of the tangential crank forces for each pedal. The tangential forces of the pedals are added up to the total tangential force exerted on the mechanical drive. The data from the measurement bicycle were obtained from Dieltiens et al. [40]. Dieltiens et al. used the data to analyse differences in cycling with and without assistance. The data of a pedal-assisted test is collected and organised according to the pedal orientation. The values are interpolated to acquire a one-degree interval from 0° to 360°. The crank positions according to time are used to calculate the angular velocity of the pedal crank. Using formula 1, the variations in the angular velocity according to the crank orientation are obtained. The measurement bicycle was set up stationary on resistance rollers. Resistance rollers are used to stationary simulate a resistance similar to natural cycling.

5.3 *Comparison method*

The generated pedal current is compared with the total tangential force of the measurement bicycle. They don't have the same unit and require a scale for comparison. The data processed according to the pedal orientation allows for the same size comparison. Furthermore, the variation in the angular velocity is compared. The combined analysis determines the differences between the pedal series hybrid and a pedal parallel hybrid. A student's T-Test is performed with the scaled current data of the pedal generator and the total tangential pedal force of the measurement bicycle. This test evaluates the significance of the resistance and the tangential force.

6. Results

All test subjects were impressed by the performance and natural feeling of the test tricycle. They stated that pedalling the tricycle feels natural once departed. They used the level of assistance just like with a conventional e-bike. They experienced uphill and full-load driving conditions. Departing from zero speed took a couple of tries to get used to it. They obviously had to get used to the unexpected behaviour: the pedals can be rotated even when the tricycle does not move yet. After some attempts, this difference from a traditional drivetrain is experienced as very favourable: almost

no force is required to depart. Furthermore, riding at a preferred rotational pedal speed is just as natural as riding on a conventional bike. About half the test subjects mentioned a difference between driving the generator and a conventional e-bike without being able to describe the difference in detail. Some of them mentioned “pushing through the resistance”. This difference is contributed to the higher gain in angular velocity around the foremost position of the crank.

The measurements selected in Figures 14 and 15 have a cadence between 50-70 rpm. This was done at a constant velocity between 15-25 kph. The selected data from [33] originate from a single level of assistance and the measurement bicycle did not shift gears.

The pedal generator data consist of 1,703 full pedal rotations and the measurement bicycle data consists of 124 full pedal rotations. The graph shows the mean ± 2 times the standard deviation of the pedal generator torque in grey and the measurement bicycle scaled tangential force in red according to the pedal orientation. 0 degree is the vertical orientation of the pedal cranks with the right pedal upwards. The force/resistance of the first peak was applied by the right leg and the second by the left leg.

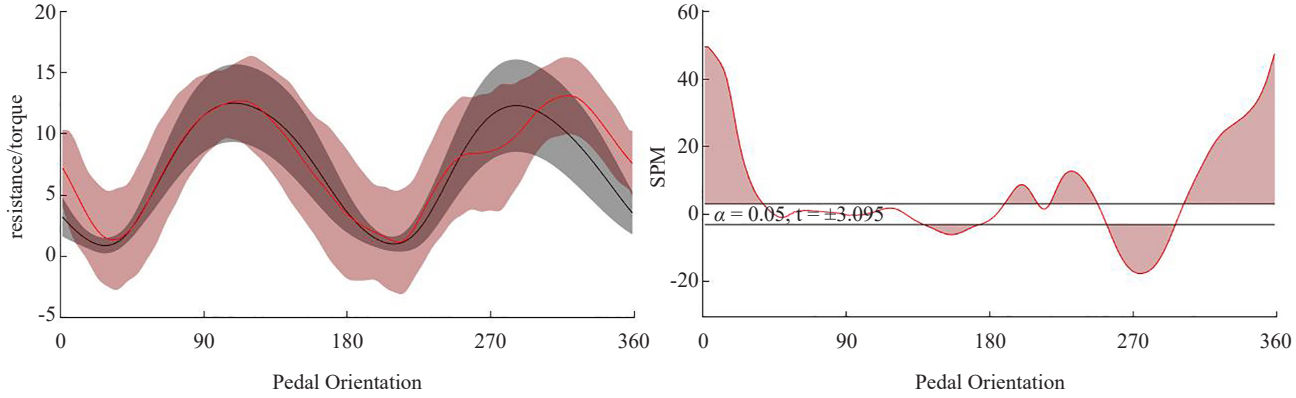

Figure 14. force/current according to orientation and T-Test results

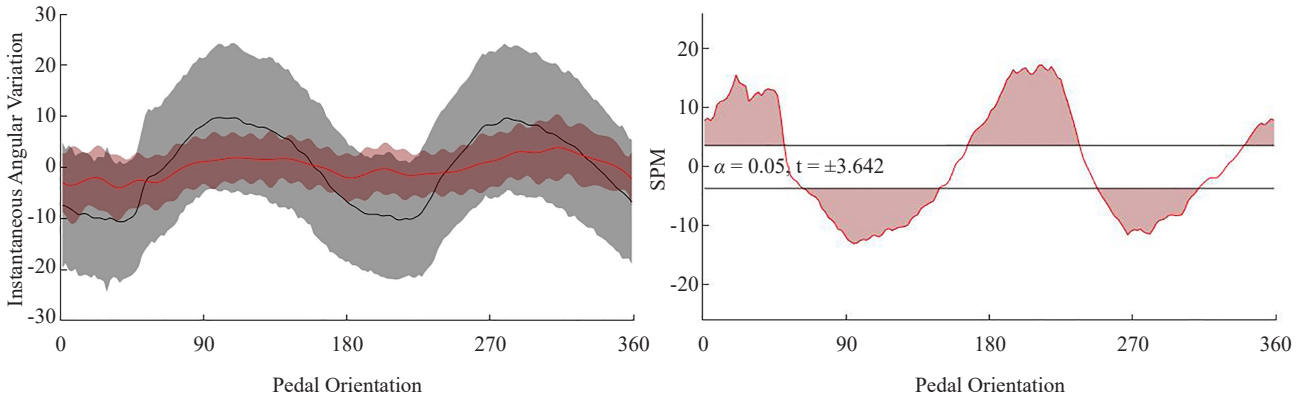

Figure 15. graph of angular velocity variations and T-Test results

7. Discussion

The tangential force of the measurement bicycle clearly shows the same behaviour compared with the pedal generator. The T-test proves the majority of the first half has 95% confidence of significance. The pedal generator has a smoother curve compared to a traditional bicycle. This is due to the control loop that controls the resistance. The

standard deviation of the pedal generator looks proportional according to the resistance. The dead centres have a low deviation as the control loop receives little input of the rotational difference between the pedal generator and the main input is the constant counter torque.

The pedal generator has a rotational speed IAV variation of ±10%. This is a significant difference compared with a traditional drivetrain. The measurement bicycle has a lower variance of ±4%. Resistance rollers have lower inertia than road cycling due to the moving mass of the bicycle and cyclist, which is not taken into account in the measurement of bicycle setup. This may have caused a higher variation in the angular velocity of the pedal crank compared to cycling on the road. Testing on the roads would have caused a greater difference. The flexible transmission of the pedal generator and the vehicle wheel results in a higher variation in the angular pedal velocity. The flexible transmission also causes a higher deviation in the variance. This variation isn't extreme as Favero noticed variations ranging from 2% to 10% [38].

The IAV variation of the angular velocity corresponds to the generated current. During the dead centres, the angular velocity is around -10% of the mean cadence and the generated current is also at its lowest. At the orientations where the pedal generator generates peak currents, the angular velocity is around +10% of the mean cadence. The rotational difference between the pedal generator and the hub motors simulates the inertia as observed during the resistance. However, due to the set proportional gain and the electrical transmission, wanting to push more on the pedal generator causes a momentary increase in the rotational speed. This effect is only slightly present on a conventional drivetrain. An increase in force has little effect on the rotational speed due to the high inertia of the vehicle and the stiff mechanical drivetrain.

There is an asymmetry present in the measurement of bicycle data that cannot be explained properly. The peaks of the left leg and the right leg have an equal maximum force, however, the peaks are 200 degrees apart. This should be 180° ± 1° [32]. Furthermore, the applied force of the left leg doesn't have the same sinusoidal shape as the right leg. The same asymmetry is present in the IAV variation of the instrumented bicycle. The peak of the right leg occurs around the same orientation while the peak created by the left leg is 20 degrees after the pedal generator. This can be due to the difference in the left and right legs of the cyclist.

8. Conclusion

The three main objectives of this research have been reached:

Test subjects experience a natural pedalling feeling when riding the test tricycle. This is confirmed by comparing pedalling data from this tricycle with data from a pedal parallel drivetrain in a conventional mid-motor e-bike. The mechanical resistance experienced by cyclists when pushing their pedals is similar to the PSHD and the conventional e-bike. Some test subjects reported an undefined difference between the tricycle and a conventional e-bike. This difference is attributed to a higher variance of the Instantaneous Angular Velocity in the PSHD, caused by the choice not to use a crank orientation measurement.

The PSHD serves as an electrical gearbox by creating a variable speed ratio between the pedal speed and the wheel speed.

The actual global driving conditions are used in the control loop for the resistance of the generator and influence the level of electrical assistance based on the electrical current in the hub motors.

Conflict of interest

The authors declare no conflicts of interest.

References

[1] J. D'Hondt, D. Degryse, P. Slaets, E. Demeester, and M. Juwet, "Handling qualities of a new last-mile vehicle," *Journal of Transportation Technologies*, vol. 12, no. 1, pp. 137-158, 2022.

[2] A. B. Kinzel, "Electrically powered cycle," United States Patent 3884317, 20 May, 1975.

[3] E. Tournon, P. Venet, B. Barbedette, A. Lelievre, J. Aubry, and A. Sari, "Efficiency comparison between series hybrid bike and traditional bike," in *Fourteenth International Conference on Ecological Vehicles and Renewable Energies (EVER)*. Monte-Carlo, Monaco, 2019, pp. 1-7.
[4] A. Fuchs, *Electronic bicycles are free of costs for (automated) mechanical transmissions*. Berne, Switzerland, 2012.
[5] S. Raghunath, *Hardware design considerations for an electric bicycle using a BLDC motor.* Texas Instruments, 2021.
[6] L. Cruces. "The arcimoto lean mean machine." Arcimoto. Available: https://www.arcimoto.com/mlm [Accessed May 11, 2022].
[7] EUR-Lex, "Regulation (EU) No 168/2013 of the European Parliament and of the Council of 15 January 2013 on the approval and market surveillance of two-or three-wheel vehicles and quadricycles," Document 32013R0168, 2013. Available: http://data.europa.eu/eli/reg/2013/168/2020-11-14 [Accessed Nov. 24, 2021].
[8] R. dot, "E-bike mando footloose," in *Reddot design award: best of the best 2013, ed. Red dot*. 2013.
[9] "Bubble post deploys new cargo bicycle for city distribution in Brussels." Gondola. Available: https://www.gondola.be/nl/news/bubble-post-zet-nieuwe-cargofiets-voor-stadsdistributiebrussel#:~:text=Sinds%20deze%20week%20gebruikt%20Bubble,andere%20steden%20zullen%20worden%20ingezet [Accessed May 10, 2022].
[10] E. Tournon, *Optimal sizing of an hybrid series bicycle equiped with supercapacitor*. University Claude Bernard Lyon 1, Lyon, 2020.
[11] E. Tournon. "The solar bike of Edgar," The Sun Trip, French, 2020. https://www.thesuntrip.com/en/participants/edgar-tournon/ [Accessed May 10, 2022].
[12] I. Lesens, "An electric bike without chain or universal joint, and without battery," (in French), Isabelle et le vélo, 2021. Available: https://www.isabelleetlevelo.fr/2021/01/05/un-velo-sans-chaine-ni-batterie-il-pourrait-revolutionner-la-mobilite-active/ [Accessed Feb. 15, 2022].
[13] B. Cauquil, "My Sun Trip 2021 in a few figures." (in French), The Sun Trip, 2021. Available: https://www.thesuntrip.com/en/mon-sun-trip-2021-en-quelques-chiffres/ [Accessed Feb. 15, 2022].
[14] B. Caquil. "Sunrider EcoMobile Baroudeur." Sunrider, 2022. Available: http://www.sunrider.fr/ [Accessed Jan. 10, 2022].
[15] P. Brunet, "Le Teil: the city is trying out an electric bicycle bus that is very popular in Europe," (in French), Le Dauphiné, 2019. Available: https://c.ledauphine.com/ardeche/2019/06/26/le-teil-la-ville-essaie-un-velobus-electrique-tres-prise-en-europe [Accessed Feb. 15, 2022].
[16] S. Cho. "Micro mobility." Mando Corp, 2017. Available: https://www.mando.com/eng/rnd/rnd05.jsp [Accessed Feb. 15, 2022].
[17] A. Schaeffler. "Schaeffler presents chainless electric drive system "Free Drive" for bicycles," Schaeffler AG, Germany, 2021. Available: https://www.schaeffler.com/en/news_media/press_releases/press_releases_detail.jsp?id=87716736 [Accessed Sep. 1, 2021].
[18] B. Borrell, "Physics on two wheels," *Nature*, vol. 535, no. 7612, pp. 338-341, 2016.
[19] A. L. Schwab, and J. P. Meijaard, "A review on bicycle dynamics and rider control," *Vehicle System Dynamics*, vol. 51, no. 7, pp. 1059-1090, 2013.
[20] J. P. Meijaard, J. M. Papadopoulos, A. Ruina, and A. L. Schwab, "Linearized dynamics equations for the balance and steer of a bicycle: A benchmark and review," *Russian Journal of Nonlinear Dynamics*, vol. 9, no. 2, pp. 343-376, 2013.
[21] J. Kooijman, and A. Schwab, "A review on handling aspects in bicycle and motorcycle control," International Design Engineering Technical Conferences and Computers and Information in Engineering Conference, 2011, pp. 597-607.
[22] T. Williams, S. Kaul, and A. Dhingra, "Influence of frame stiffness and rider position on bike dynamics: Analytical study," presented at the ASME 2015 International Mechanical Engineering Congress and Exposition, Houston, Texas, USA, 2015.
[23] J. Xiong, N. Wang, and C. Liu, "Stability analysis for the Whipple bicycle dynamics," *Multibody System Dynamics*, vol. 48, no. 3, pp. 311-335, 2020.
[24] S. Dieltiens, J. D'hondt, M. Versteyhe, and M. Juwet, "Theoretical self-stability of E-bikes," in *42nd Congress of the Biomechanical Society*. Reims, France, 2017.
[25] J. D. G. Kooijman, J. P. Meijaard, J. M. Papadopoulos, A. Ruina, and A. L. Schwab, "A bicycle can be self-stable without gyroscopic or caster effects," *Science*, vol. 332, no. 6027, pp. 339-342, 2011.
[26] S. Dieltiens, J. D'Hondt, M. Juwet, K. Shariatmadar, and M. Versteyhe, "Design and calibration of an instrumented seat post to measure sitting loads while cycling," *Sensors*, vol. 20, no. 5, pp. 1384, 2020.

[27] J. D'Hondt, S. Dieltiens, M. Juwet, and M. Versteyhe, "Design and calibration of a 6-component balance on a bicycle steer," *Proceedings of the Eighteenth International Conference of Experimental Mechanics*, vol. 2504-3900, pp. 520, 2018.
[28] D. Krumm, and S. Odenwald, "Development of a dynamometer to measure grip forces at a bicycle handlebar," *Procedia Engineering*, vol. 72, pp. 80-85, 2014.
[29] S. Dieltiens, J. D'Hondt, M. Juwet, and M. Versteyhe, "Development of a low-cost measurement system to determine 3-dimensional pedal loads during in-situ cycling," *Transport Problems*, vol. 14, no. 4, pp. 151-159, 2019.
[30] S. Dorel, A. Couturier, J.-R. Lacour, H. Vandewalle, C. Hautier, and F. Hug, "Force-velocity relationship in cycling revisited," *Medicine and Science in Sports and Exercise*, vol. 42, no. 6, pp. 1174-1183, 2010.
[31] F. Bolourchi, and M. Hull, "Measurement of rider induced loads during simulated bicycling," *International Journal of Sport Biomechanics*, vol. 1, no. 4, pp. 308-329, 1985.
[32] R. Bini, P. Hume, and A. Cerviri, "A comparison of cycling SRM crank and strain gauge instrumented pedal measures of peak torque, crank angle at peak torque and power output," *Procedia Engineering*, vol. 13, pp. 56-61, 2011.
[33] G. Mornieux, K. Zameziati, E. Mutter, R. Bonnefoy, and A. Belli, "A cycle ergometer mounted on a standard force platform for three-dimensional pedal forces measurement during cycling," *Journal of Biomechanics*, vol. 39, no. 7, pp. 1296-1303, 2006.
[34] R. R. Davis, and M. Hull, "Measurement of pedal loading in bicycling: II. Analysis and results," *Journal of Biomechanics*, vol. 14, no. 12, pp. 857-872, 1981.
[35] N. A. Turpin, and B. Watier, "Cycling biomechanics and its relationship to performance," *Applied Sciences*, vol. 10, no. 12, pp. 1-15, 2020.
[36] F. Höchtl, H. Böhm, and V. Senner, "Prediction of energy efficient pedal forces in cycling using musculoskeletal simulation models," *Procedia Engineering*, vol. 2, no. 2, pp. 3211-3215, 2010.
[37] Favero Electronics srl, *Advantages of the IAV power system*. Favero Electronics SRL, 2022.
[38] Favero Electronics srl, *Influence of angular velocity of pedaling on the accuracy of the measurement of cyclist power*. Favero Electronics SRL, 2018.
[39] J. D'hondt, M. Juwet, E. Demeester, and P. Slaets, "Development of an electric tricycle for service companies and last-mile parcel delivery," *Transport Problems*, vol. 17, no. 2, pp. 175-187, 2022.
[40] S. Dieltiens, C. Jiménez-Peña, S. Van Loon, J. D'hondt, K. Claeys, and E. Demeester, "Influence of electrically powered pedal assistance on user-induced cycling loads and muscle activity during cycling," *Applied Sciences*, vol. 11, no. 5, pp. 2032, 2021.